Invited Review Paper

Bifurcation Analysis of a Class of Generalized Hénon Maps with Hidden Dynamics

Seiya Amoh[*a)] Non-member, Xu Zhang[**] Non-member
Guanrong Chen[***] Non-member, Tetsushi Ueta[*] Non-member

(Manuscript received April 23, 2021, revised August 20, 2021)

Although continuous systems such as the Chua circuit are known as systems with hidden attractors, hidden attractors also exist in classical discrete maps, such as a generalized Hénon map. A hidden attractor is an attractor that does not overlap with its own attracting region in its vicinity, which makes it difficult to visualize. In this paper, a local bifurcation analysis method for discrete maps is described, and the bifurcation analysis of the generalized Hénon map is performed using the method. The bifurcation structure, as the parameters are changed, shows a certain law, and the interesting Neimark-Sacker bifurcation and period-doubling bifurcation are confirmed to occur simultaneously. It was also found that the hidden attractors exist in the rectangular characteristic chaotic regions, and they appear relatively frequently near the window of chaos.

Keywords: Hidden attractor, Bifurcation analysis, Chaos

1. Introduction

Consider the n-dimensional discrete dynamical system:

$$\begin{aligned} &\boldsymbol{x}_{k+1} = \boldsymbol{f}(\boldsymbol{x}_k, \lambda), \\ &\boldsymbol{f} : \boldsymbol{R}^n \to \boldsymbol{R}^n,\ \boldsymbol{x}_k \in \boldsymbol{R}^n, \lambda \in \boldsymbol{R}, \end{aligned} \tag{1}$$

where $\boldsymbol{x}_k$ is the state and λ is a parameter. The iteration of a discrete dynamical system could be related to chaos theory, which has been a focal topic of intensive research since the discoveries of the Lorenz attractor and Li-Yorke chaos [(1)] [(2)] [(3)].

For a point $\boldsymbol{x}_0 \in \boldsymbol{R}^n$, if there is a positive integer ℓ such that

$$\boldsymbol{f}^\ell(\boldsymbol{x}_0, \lambda) = \boldsymbol{x}_0, \tag{2}$$

where $\boldsymbol{f}^\ell = \overbrace{\boldsymbol{f} \circ \boldsymbol{f} \circ \cdots \circ \boldsymbol{f}}^{\ell}$, then $\boldsymbol{x}_0$ is called a periodic point with period ℓ. In particular, for $\ell = 1$, $\boldsymbol{x}_0$ is a fixed point.

A compact region $V \subset \boldsymbol{R}^n$ is called a trapping region provided that $\boldsymbol{f}(V)$ is contained in the interior of V. A set Λ is called an attracting set if there is a trapping region V such that

$$\Lambda = \bigcap_{k \geq 0} \boldsymbol{f}^k(V).$$

A set Λ is called an attractor provided that it is an attracting set which is nontrivial if the $\boldsymbol{f}$ restricted to Λ has complex dynamics (for example, $\boldsymbol{f}$ has sensitive dependence on initial conditions or positive Lyapunov exponents on Λ).

For dynamical system (1), bifurcation analysis means the study of the qualitative change of the dynamics with the variation of some parameters. For a fixed point $\boldsymbol{x}_0$ with a fixed parameter λ_0, i.e., $\boldsymbol{f}(\boldsymbol{x}_0, \lambda_0) = \boldsymbol{x}_0$, there are several types of bifurcations, such as saddle-node bifurcation, period-doubling bifurcation (or flip bifurcation), Andronov-Hopf bifurcation, and so on. For more information, please refer to [(4)].

For discrete dynamical systems, two well-known systems with chaotic dynamics are the Logistic map and the Hénon map, which are polynomial functions brought forward by May [(5)] and Hénon [(6)], respectively. Polynomial maps are important models in discrete dynamical systems because of their simple expressions with complicated dynamical behaviors.

In particular, the Hénon map or a generalized Hénon map is an important model of two-dimensional polynomial diffeomorphic maps defined on $\boldsymbol{R}^2$. The parameter region for the existence of chaotic dynamics for the real quadratic Hénon map was studied by Devaney and Nitecki [(7)]. An interesting result is that the polynomial diffeomorphic map with a constant Jacobian from the real or complex plane to itself is either conjugate to a composition of generalized Hénon maps or dynamically trivial, as shown by Friedland and Milnor [(8)]. The real cubic Hénon map was considered by Dullin and Meiss [(9)]. Some comprehensive characterizations between the dynamical behavior and the parameters for the real Hénon map were obtained respectively by Benedicks, Carleson, Viana, and Young et al. [(10)] [(11)] [(12)].

Techniques from complex dynamics were used by Bedford and Smillie [(13)] [(14)] to show the existence of chaotic dynamics and a quadratic tangency between stable and unstable manifolds of fixed points for the real Hénon map under certain conditions. The existence of chaotic dynamics and an orbit of tangency for the Hénon-like families of diffeomorphisms on the real plane were obtained by Cao et al. [(15)] using real

a) Correspondence to: c502147001@tokushima-u.ac.jp
[*] Graduate School of Tokushima University, 770-8506, Tokushima, Japan
[**] xu_zhang_sdu@mail.sdu.edu.cn, Department of Mathematics, Shandong University, Weihai 264209, Shandong, China
[***] eegchen@cityu.edu.hk, Department of Electrical Engineering, City University of Hong Kong, Hong Kong SAR, China

analytic methods. The parameter regions for the existence of chaotic dynamics of some generalized Hénon maps were investigated by Zhang [16].

On the other hand, a continuous dynamical system is defined by an ordinary differential equation, as $d\boldsymbol{x}/dt = \Phi(\boldsymbol{x})$ with $\boldsymbol{x} \in \boldsymbol{R}^n$ and $\Phi : \Omega \subset \boldsymbol{R}^n \to \boldsymbol{R}^n$. An equilibrium is a real solution to $\Phi(\boldsymbol{x}) = \boldsymbol{0}$. Generally, there are two types of continuous chaotic systems according to their different types of equilibria, namely systems with self-excited attractors and systems with hidden attractors. For a system with an attractor, if the basin of attraction intersects with arbitrarily small neighborhoods of an equilibrium, then the attractor is classified as self-excited, and the corresponding system is called a self-excited system. Otherwise, the system is said to have a hidden attractor [17]. For example, the chaotic Lorenz system [2] and the chaotic Chen system [18] with the classical parameters are self-excited, while the Chua circuit with a chaotic attractor could be hidden for some particular parameter values [19]. In the studies of continuous dynamical systems, there are many results on various systems with hidden attractors [20] [21] [22] [23].

Intuitively, discrete dynamical systems with hidden attractors can be similarly defined and studied. However, the study of discrete systems with hidden attractors received much less attention. Jafari et al. [24] demonstrated the existence of some hidden attractors in one-dimensional maps by extending the analysis on the Logistic map. Jiang et al. [25] studied a class of two-dimensional quadratic maps with hidden attractors. Zhang and Chen [26] studied a class of generalized Hénon maps and showed the coexistence of an attracting fixed point and a hidden attractor, and the existence of Smale horseshoe for a subshift of finite type and also Li-Yorke chaos.

It is noted that, in [26], only part of the parameter region was analyzed, leaving many interesting problems for further studies. In this article, we carry out more detailed analysis of the generalized Hénon map. We study its bifurcations in different parameter regions: tangent, period-doubling, and Neimark-Sacker bifurcations, via careful numerical simulations, unveiling some new dynamical phenomena such as the coexistence of two attractors, namely an attracting fixed point and a hidden attractor, where the hidden attractor is either a periodic orbit or a strange attractor depending on the parameter values.

2. Local bifurcation analysis method

In this section, a numerical method is introduced to compute local bifurcation sets for the given discrete system (2).

First, consider an ℓ-periodic fixed point $\boldsymbol{x}^*$. The fixed point satisfies the following equation:

$$\boldsymbol{f}^\ell(\boldsymbol{x}^*) - \boldsymbol{x}^* = \boldsymbol{0}. \tag{3}$$

With a small perturbation $\boldsymbol{\xi} \in \boldsymbol{R}^n$, the Taylor expansion around a fixed point is

$$\begin{aligned} \boldsymbol{x}_{(k+1)} &= \boldsymbol{x}^* + \boldsymbol{\xi}_{(k+1)} \\ &= \boldsymbol{f}^\ell(\boldsymbol{x}^*) + \left.\frac{\partial \boldsymbol{f}^\ell}{\partial \boldsymbol{x}}\right|_{\boldsymbol{x}=\boldsymbol{x}^*} \boldsymbol{\xi}_{(k)} + \cdots \end{aligned} \tag{4}$$

Neglecting the higher-order terms, from Eq.(4), one has

$$\boldsymbol{\xi}_{(k+1)} = \left.\frac{\partial \boldsymbol{f}^\ell}{\partial \boldsymbol{x}}\right|_{\boldsymbol{x}=\boldsymbol{x}^*} \boldsymbol{\xi}_{(k)}. \tag{5}$$

Therefore, since the difference equation near the fixed point is expressed by Eq.(5), the stability of the fixed point can be discussed by the eigenvalues μ_i of the Jacobian matrix $\partial \boldsymbol{f}^\ell/\partial \boldsymbol{x}$. The characteristic equation is written as follows:

$$\chi(\mu) = \det\left(\frac{\partial \boldsymbol{f}^\ell}{\partial \boldsymbol{x}} - \mu I_n\right) = 0. \tag{6}$$

By convention, the eigenvalues of the Jacobian matrix in the linearized space of the difference equation are called characteristic constants μ_i, which will be followed. The expressions of the stability of a fixed point are summarized in Table.1. The ℓ-periodic stable fixed point is denoted by ${}_0D^\ell$.

Table 1. Classification of the stability of fixed points in 2-dimensional discrete systems.

Stability	Symbol	Multiplier
Completely stable	${}_0D$	$\lvert\mu_1\rvert < 1, \lvert\mu_2\rvert < 1$
Directly unstable	${}_1D$	$0 < \mu_1 < 1 < \mu_2$
Inversely unstable	${}_1I$	$\mu_1 < -1 < \mu_2 < 0$
Completely unstable	${}_2D$	$\lvert\mu_1\rvert > 1, \lvert\mu_2\rvert > 1$

In a discrete system, a bifurcation phenomenon occurs when the characteristic constant of the Jacobian matrix near a fixed point satisfies $|\mu_i| = 1$. Bifurcation phenomena in discrete systems can be classified into three categories: tangent bifurcation for $\mu_i = 1$, period-doubling bifurcation for $\mu_i = -1$, and Neimark-Sacker bifurcation for $\mu_i = e^{j\theta}, \theta \neq 0, \pi$, where θ is the argument.

To compute the bifurcation set, it is sufficient to solve Eq.(3) and Eq.(6), in which the characteristic constants corresponding to each bifurcation condition are substituted. In this study, Newton's method is used because of its good convergence ability.

The Jacobian matrix required to solve Eq.(3) by Newton's method is

$$\begin{pmatrix} \dfrac{\partial \boldsymbol{f}^\ell}{\partial \boldsymbol{x}} - I_n & \dfrac{\partial \boldsymbol{f}^\ell}{\partial \lambda} \\ \dfrac{\partial \chi(\mu)}{\partial \boldsymbol{x}} & \dfrac{\partial \chi(\mu)}{\partial \lambda} \end{pmatrix}. \tag{7}$$

Note that $\boldsymbol{f}^\ell = \overbrace{\boldsymbol{f} \circ \boldsymbol{f} \circ \cdots \circ \boldsymbol{f}}^{\ell}$. Derivatives about $\boldsymbol{f}$ are given as follows:

$$\begin{aligned} \frac{\partial \boldsymbol{f}^\ell}{\partial \boldsymbol{x}} &= \prod_{k=0}^{\ell-1} \left.\frac{\partial \boldsymbol{f}}{\partial \boldsymbol{x}}\right|_{\boldsymbol{x}=\boldsymbol{x}_{(\ell-k)}}, \\ \frac{\partial \boldsymbol{f}^\ell}{\partial \lambda}(\boldsymbol{x}_{\ell-1}) &= \frac{\partial \boldsymbol{f}}{\partial \boldsymbol{x}}(\boldsymbol{x}_{\ell-1})\frac{\partial \boldsymbol{f}^{\ell-1}}{\partial \lambda}(\boldsymbol{x}_{\ell-1}) + \frac{\partial \boldsymbol{f}}{\partial \lambda}(\boldsymbol{x}_{\ell-1}), \\ \frac{\partial \boldsymbol{f}^j}{\partial \lambda}(\boldsymbol{x}_{j-1}) &= \frac{\partial \boldsymbol{f}}{\partial \boldsymbol{x}}(\boldsymbol{x}_{j-1})\frac{\partial \boldsymbol{f}^{j-1}}{\partial \lambda}(\boldsymbol{x}_{j-1}) + \frac{\partial \boldsymbol{f}}{\partial \lambda}(\boldsymbol{x}_{j-1}), \\ \frac{\partial \boldsymbol{f}^1}{\partial \lambda}(\boldsymbol{x}_0) &= \frac{\partial \boldsymbol{f}}{\partial \lambda}(\boldsymbol{x}_0), \end{aligned} \tag{8}$$

where $\boldsymbol{x}_k = \boldsymbol{f}^k(\boldsymbol{x}_0)$. Derivatives of the characteristic equation requires the second-order derivative of the map $\boldsymbol{f}^\ell$, which is omitted here because of the complicated form of the equation.

Now, we are ready to compute the bifurcation set of n-dimensional discrete systems.

3. Bifurcation analysis of Generalized Hénon maps

Consider the generalized Hénon map [26]:

$$\begin{cases} x_{k+1} = dy_k \\ y_{k+1} = P(y_k) + cx_k, \end{cases} \tag{9}$$

where $P(x) = ax^m(x^2 - b^2), m \in \boldsymbol{N}$. By checking the dynamic behavior roughly in advance, a seems to be an essential parameter for bifurcations. Let us fix $b = 1.0$ and $c = 0.005$.

The bifurcation calculation is performed with a as the variable parameter and d as the incremental parameter. Also, following Theorems 4.1 and 4.4 in Ref. [26], the range of the bifurcation calculation is ensured to be $a > 0$, $0 < d \leq 1$.

The Jacobian matrices required for the Newton method are

$$\frac{\partial \boldsymbol{f}}{\partial \boldsymbol{x}} = \begin{pmatrix} 0 & d \\ c & amy^{m-1}(y^2 - b^2) + 2ay^{m+1} \end{pmatrix}, \frac{\partial^2 \boldsymbol{f}}{\partial \boldsymbol{x} \partial x} = \begin{pmatrix} 0 & 0 \\ 0 & 0 \end{pmatrix},$$
$$\frac{\partial^2 \boldsymbol{f}}{\partial \boldsymbol{x} \partial y} = \begin{pmatrix} 0 & 0 \\ 0 & a(m^2 - m)y^{m-2}(y^2 - b^2) + 2a(2m+1)y^m \end{pmatrix},$$
$$\frac{\partial \boldsymbol{f}}{\partial a} = \begin{pmatrix} 0 \\ y^m(y^2 - b^2) \end{pmatrix}, \frac{\partial^2 \boldsymbol{f}}{\partial \boldsymbol{x} \partial d} = \begin{pmatrix} 0 & 0 \\ 0 & my^{m-1}(y^2 - b^2) + 2y^{m+1} \end{pmatrix}. \tag{10}$$

Figure 1 shows two stable fixed points of the map with $m = 2, a = 3.16, d = 0.5$. One stable fixed point at the origin (a) and one stable fixed point in the third quadrant (b) are generated. These fixed points are bistable, but bifurcation phenomena occur only for (b).

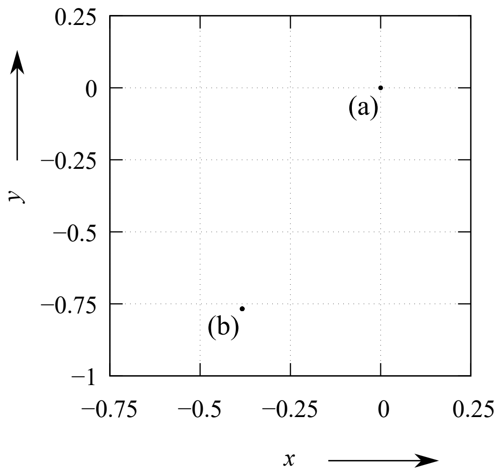

Fig. 1. Two stable fixed points when $m = 2, a = 3.16, d = 0.5$.

Figure 2 shows the bifurcation diagram when $m = 2$, where white lines are bifurcation sets calculated by Newton's method. This bifurcation diagram includes the classification of periods by colors, which is obtained by the exhaustive searching method. Although the this method cannot find multiple attractors simultaneously, bifurcation sets and consequent analyses give supplementary information on topological consistency about saddle periodic points and multistability. The colors in the bifurcation diagrams are assigned according to the number of period i.e., 1:blue, 2:red, 3:magenta, 4:green, 6:yellow, 8:slate blue, 16:purple, chaos or explosion:black.

By increasing a in the bifurcation diagram, the stable fixed point (b) : ${}_0D$ is generated by the tangent bifurcation G, and the process of chaos generation by period-doubling cascade is confirmed.

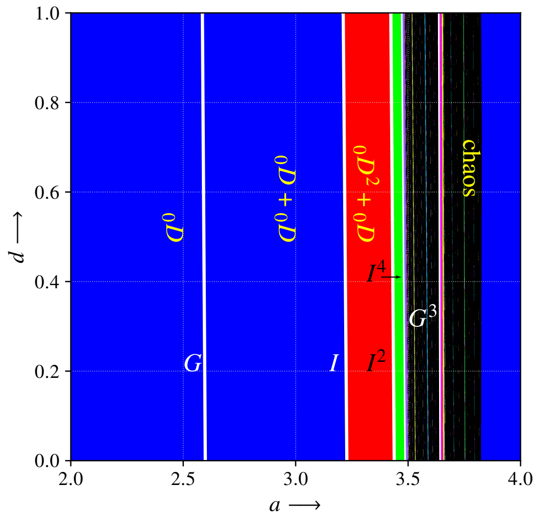

Fig. 2. The local bifurcation diagram when $m = 2$.

Figure 3 shows two stable fixed points when $m = 3, a = 4.5, d = 0.5$. In this case, unlike $m = 2$, a stable origin (a) and a stable 2-period point (b) are generated.

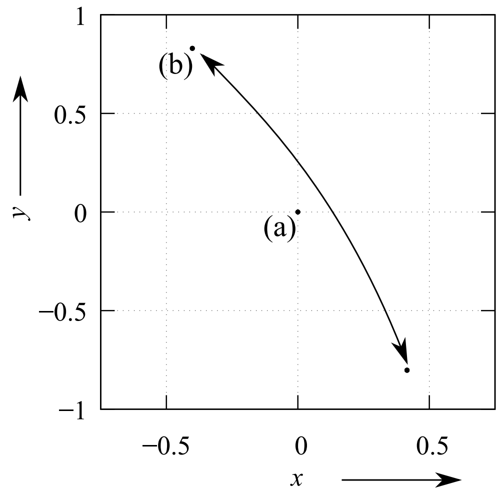

Fig. 3. Two stable fixed points when $m = 3$.

Figure 4 shows the bifurcation diagram when $m = 3$. The bifurcation structure is very similar to that of $m = 2$. The 2-period fixed point (b) : ${}_0D^2$ generated by the tangent bifurcation G^2. When a increases, another 2-period fixed point is generated by the tangential bifurcation G^2 again, and then the two 2-period fixed points $2 \times {}_0D^2$ simultaneously undergo period-doubling bifurcation and change to chaotic attractors. This means that a chaotic attractor is composed of two attractors that are merged together. This is called as “double period-doubling” [26].

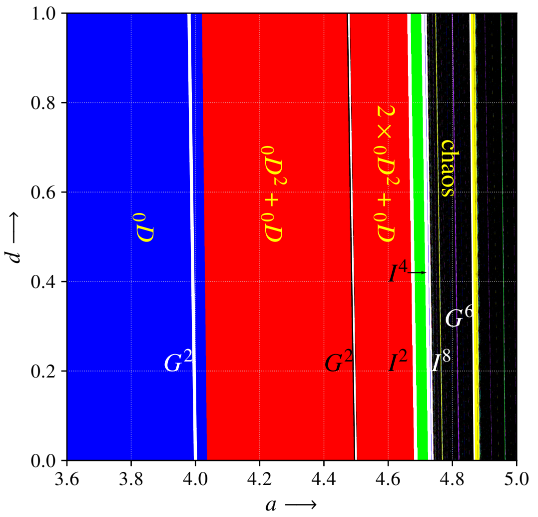

Fig. 4. The local bifurcation diagram when $m = 3$.

Figure 5 shows the chaotic hidden attractor when $m = 3, a = 5.0, d = 0.5$.

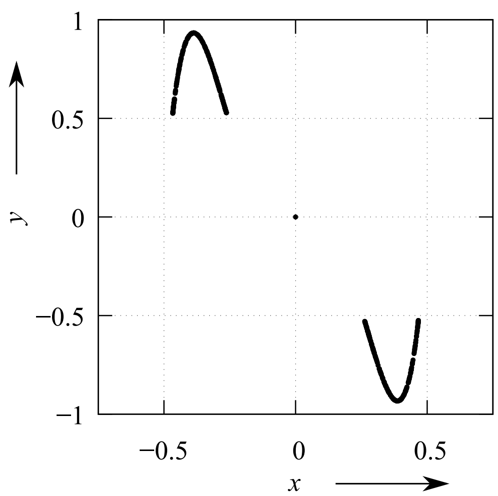

Fig. 5. The chaotic hidden attractor when $m = 3, a = 5.0, d = 0.5$.

For the case of $m = 4$, Fig.6 shows exactly the same bifurcation structure as $m = 2$. It also has a stable origin and a stable fixed point in the third quadrant, with the process of chaos generation by period-doubling bifurcation.

4. Bifurcation analysis with $P(x_k)$

Consider the generalized Hénon map [26] with $P(x_k)$:

$$\begin{cases} x_{k+1} = dy_k \\ y_{k+1} = P(x_k) + cx_k. \end{cases} \tag{11}$$

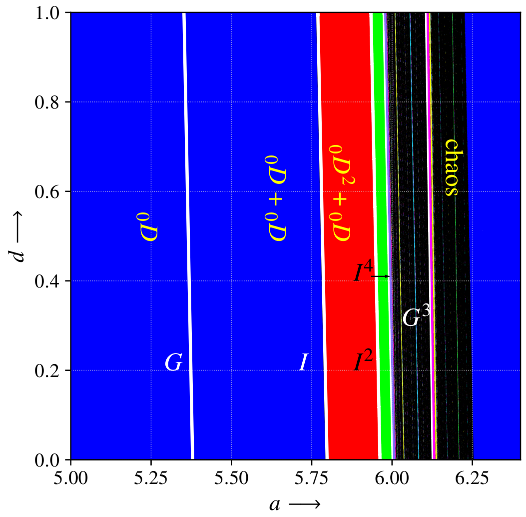

Fig. 6. The local bifurcation diagram when $m = 4$.

Although this system is effectively a one-dimensional difference equation by substituting the first equation into the second equation, a richer bifurcation phenomenon is observed than those from Eq.(9). In addition, when $m = 3$, a hidden attractor can be found in the rectangular chaotic attractor region.

Figure 7 shows the three stable fixed points when $m = 2$. The fixed point in (a) is the stable origin, while (c) shows a 1-periodic fixed point. Fixed points in (b) is 2-periodic. These fixed points exist simultaneously, especially (b) and (c) generate chaos through period-doubling cascade.

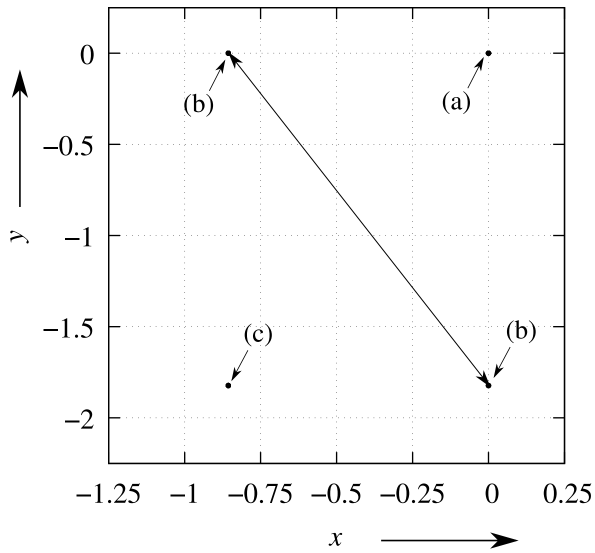

Fig. 7. Three stable periodic fixed points when $m = 2$, $a = 4.5, b = 1.02, c = 1.04, d = 0.4699$.

Now, the parameter d is treated as a variable in the bifurcation computation. Then, Jacobian matrices required for Newton’s method are

$$\frac{\partial \boldsymbol{f}}{\partial \boldsymbol{x}} = \begin{pmatrix} 0 & d \\ amx^{m-1}(x^2 - b^2) + 2ax^{m+1} + c & 0 \end{pmatrix},$$
$$\frac{\partial^2 \boldsymbol{f}}{\partial \boldsymbol{x} \partial x} = \begin{pmatrix} 0 & 0 \\ am(m-1)x^{m-2}(x^2 - b^2) + 4amx^m + 2ax^m & 0 \end{pmatrix},$$
$$\frac{\partial^2 \boldsymbol{f}}{\partial \boldsymbol{x} \partial y} = \begin{pmatrix} 0 & 0 \\ 0 & 0 \end{pmatrix}, \ \frac{\partial \boldsymbol{f}}{\partial d} = \begin{pmatrix} y \\ 0 \end{pmatrix}, \ \frac{\partial^2 \boldsymbol{f}}{\partial \boldsymbol{x} \partial d} = \begin{pmatrix} 0 & 1 \\ 0 & 0 \end{pmatrix}. \tag{12}$$

Figure 8 shows the bifurcation diagram of Eq.(11) when $m = 2$.

In the lower-left area of the figure, there is only one stable ${}_0D$ at the origin, but changing the parameter will generate fixed points (b) and (c) through tangent bifurcation G. These fixed points lead to chaos through cascade of period-doubling bifurcation I. Let the set be represented as $NS + I$. On this bifurcation set, 2-periodic fixed point ${}_0D^2$ (b) generates period-doubling bifurcation, and 1-periodic fixed point ${}_0D$ (c) generates Neimark-Sacker bifurcation, and changes to 4-periodic fixed points ${}_0D^4$ simultaneously. It should be noted that although there are multiple attractors that cause bifurcation, all these have bifurcation sets at the same positions. This also appears in the case of $m = 3$ to be discussed later.

During G and $NS + I$, (b) and (c) are merged. Like the red area at the top left of the bifurcation map, there is a part where the bifurcation set cannot be confirmed on the color boundary. This is because the exhaustive searching algorithm tracks another attractor, and there is actually no bifurcation set.

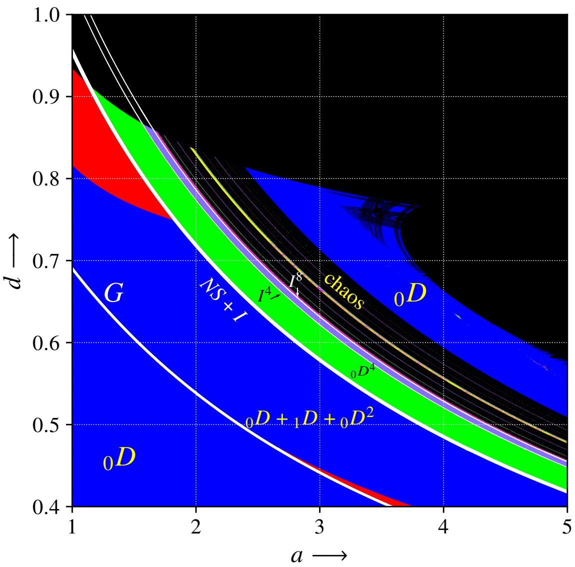

Fig. 8. The local bifurcation diagram where $m = 2$, $b = 1.02$, $c = 1.04$.

Figures 9 and 10 show examples of a 4-periodic attractor and a chaotic attractor. From Fig. 7, a period-doubling bifurcation occurs in (b), and a Neimark-Sacker bifurcation occurs in (c), with 4-periodic fixed points appearing simultaneously.

Figure 11 shows the bifurcation diagrams when $m = 3$. The bifurcation diagrams are similar to those for $m = 2$, where the 1-periodic fixed point goes through the process

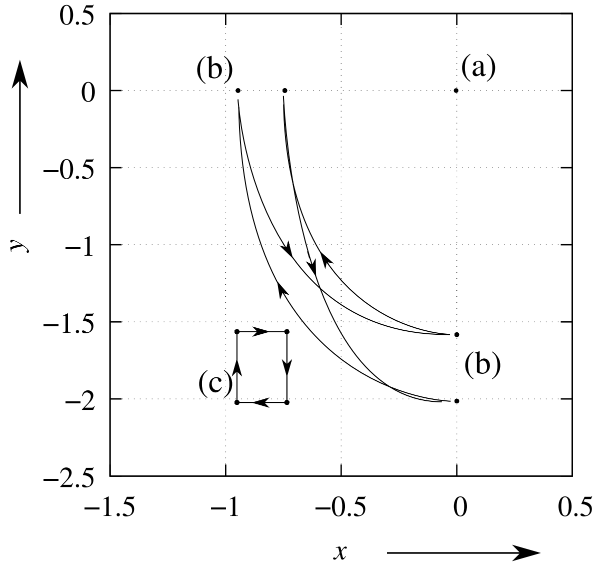

Fig. 9. 4-periodic attractor when $m = 2$, $a = 4.6$, $d = 0.4699$.

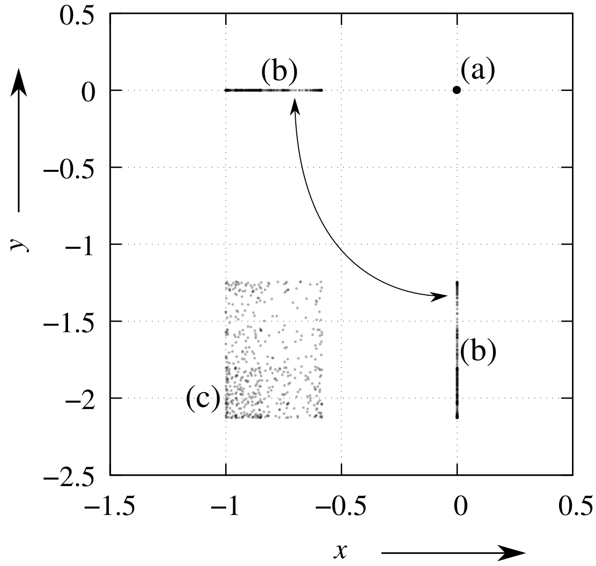

Fig. 10. Chaotic attractor when $m = 2$, $a = 4.81$, $d = 0.4699$.

of 4-periodization via the Neimark-Sacker bifurcation and chaos generation via the period-doubling cascade. In addition, it is found that there is a hidden attractor in the region of chaotic attractor for $m = 3$.

Figure 12 shows the basic periodic attractor for $m = 3$. Unlike the $m = 2$ case, it exhibits a prominent symmetry structure and a 2-periodic attractor (d):${}_0D^2$, which is not on the x-axis and y-axis. The other attractors are the same as that for $m = 2$: (a) : ${}_0D$ is the stable origin, (b) : ${}_0D^2$ is a 2-periodic fixed point on the two axes, and (c) : ${}_0D$ is a 1-periodic fixed point at which the Neimark-Sacker bifurcation occurs. Each attractor causes bifurcation at the same time as described above, and turns into a chaotic attractor as shown in Fig. 13.

Note that the red attractor in the chaotic region is a hidden attractor, which can be observed by giving a large initial value, because there is no attraction region near the hidden

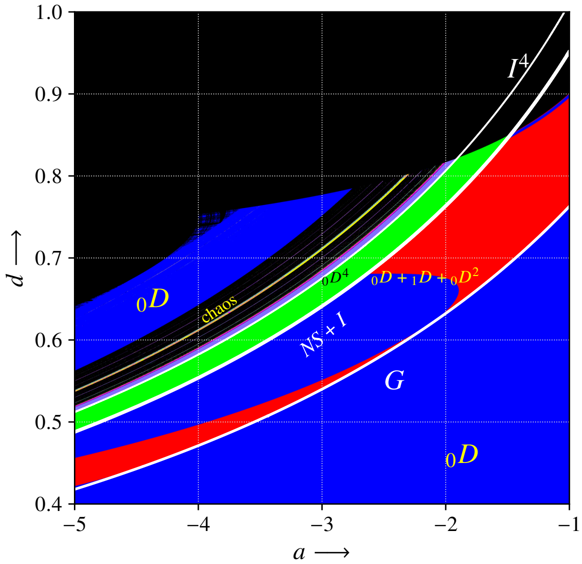

Fig. 11. The local bifurcation diagram when $m = 3$, $b = 1.02$, $c = 1.04$.

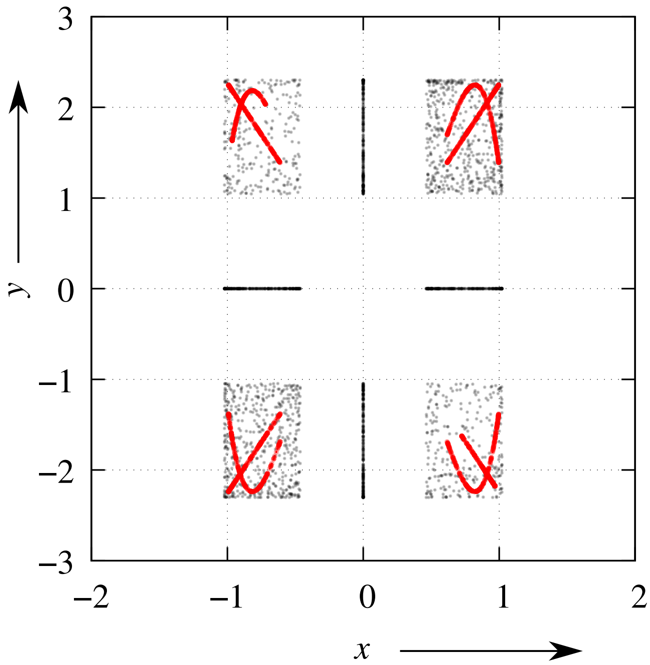

Fig. 13. Hidden attractors in chaos region when $m = 3$, $c = 1.04$, $d = 0.443336$.

attractor. However, the hidden attractor often appears clearly when crossing the window of chaos in the parameter plane. The window of chaos is bounded by the set of tangent and period-doubling bifurcations at the fixed point, and it is especially noticeable when crossing the tangent bifurcation.

More interestingly, although the chaotic attractor originates from only one fixed point (c) and (d), several more periodic attractors appear in the chaotic window. It seems that any one of the several stable fixed points in this chaotic region is closely related to the hidden attractor.

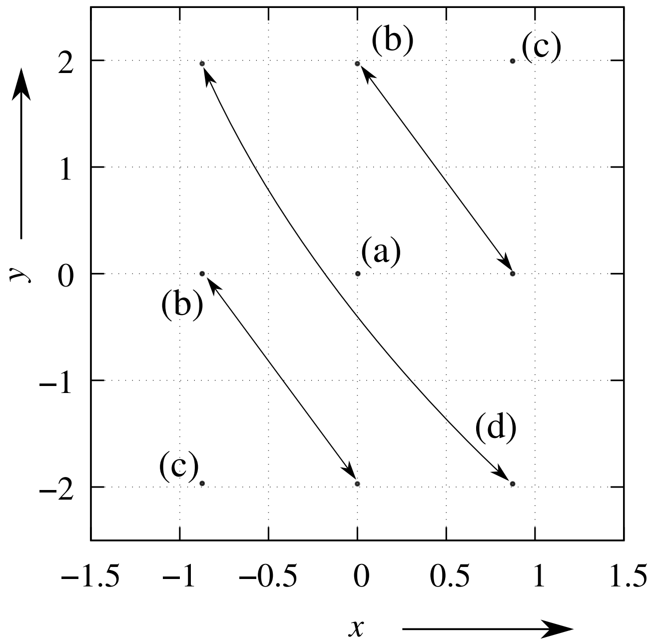

Fig. 12. Three stable periodic fixed point when $m = 3$, $a = -5.7463$, $d = 0.443346$.

Figures 14 and 15 show the bifurcation diagram when $m = 4$, and the phase portrait. In this case, the feature of multiple attractors at the same time with $m = 2, 3$ is not observed, but only one fixed point changes to a 4-period fixed point via the Neimark-Sacker bifurcation, and then the transition to chaos through the period-doubling cascade is confirmed.

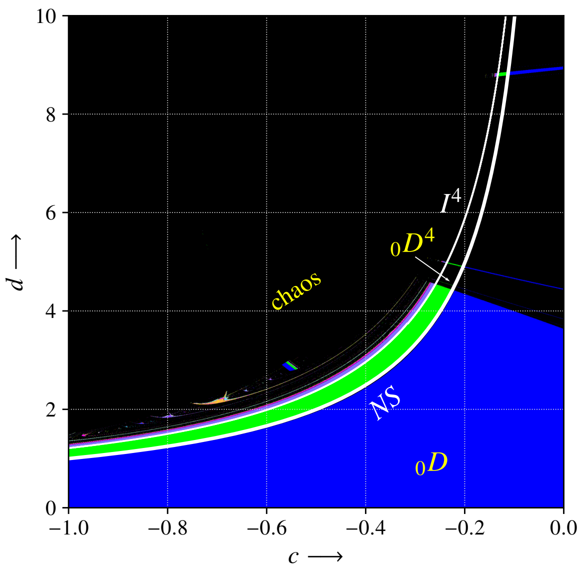

Fig. 14. The local bifurcation diagram when $m = 4$, $a = -4.4537$, $b = 1.02$.

In particular, the argument θ of the characteristic constant on the Neimark-Sacker bifurcation set is always $\theta = \pm\pi/2$, regardless of the number of m. In other words, in Eq.(11), for any m, the fixed point (c) becomes 4-periodic fixed points via

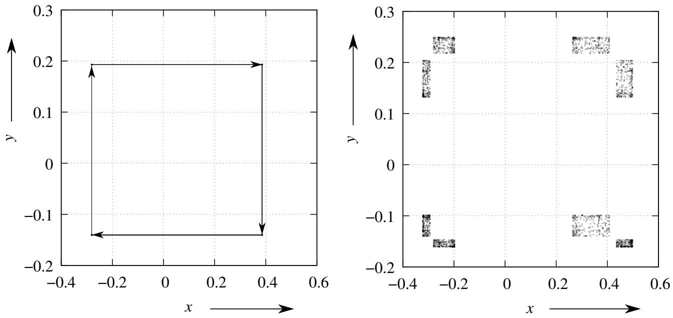

4-period, $c = -0.592$. Chaotic attractor, $c = -0.612$.

Fig. 15. Phase portrait of the fixed point (c) when $m = 4, a = -4.4537, b = 1.02, d = 2.0$.

the Neimark-Sacker bifurcation, and then chaos is expected via the period-doubling cascade.

5. Conclusion

In this paper, we calculate and analyze local bifurcations of the generalized Hénon map and its hidden attractor. In all the cases of $m = 2, 3, 4$, the mechanism of chaos generation through period-doubling cascade is confirmed. We found that the chaotic hidden attractor has the same process of chaos development as an ordinary strange attractor, although the attraction region is small. We also analyze the generalized Hénon map with $P(x_k)$. As a result, in all cases of $m = 2, 3, 4$, the mechanisms of generating chaos through the cascade of 4-periodization of fixed points and period-doubling bifurcation by $NS + I$ are clarified. Double period-doubling [26] is also confirmed for every m, and we also found that multiple attractors exist separately and bifurcate simultaneously via parameter changes. In particular, in the process of the dynamic change caused by the parameter change, two separate attractors coexist in the chaotic window, one is a chaotic attractor due to self-excited oscillation, and the other is a stable hidden attractor covered by the former one.

References

(1) T. Li and J. A. Yorke. Period three implies chaos. *Am. Math. Mon.*, 82:985–992, 1975.

(2) E. Lorenz. Deterministic non-periodic flow. *J. Atmos. Sci.*, 20:130–141, 1963.

(3) C. Sparrow. *The Lorenz Equations: Bifurcations, Chaos, and Strange Attractors*. Springer-Verlag, NY, 1982.

(4) C. Robinson. *Dynamical Systems: Stability, Symbolic Dynamics and Chaos*. CRC Press, Florida, 1999.

(5) R. May. Simple mathematical models with very complicated dynamics. *Nature*, 261:45–67, 1976.

(6) M. Hénon. A two-dimensional mapping with a strange attractor. *Commun. Math. Phys.*, 50:69–77, 1976.

(7) R. L. Devaney and Z. Nitecki. Shift automorphisms in the Hénon mapping. *Commun. Math. Phys.*, 67:137–146, 1979.

(8) S. Friedland and J. Milnor. Dynamical properties of plane polynomial automorphisms. *Ergod. Th. & Dynam. Sys.*, 9:67–99, 1989.

(9) H. R. Dullin and J. D. Meiss. Generalized Hénon maps: The cubic diffeomorphisms of the plane. *Phys. D*, 143:262–289, 2000.

(10) M. Benedicks and L. Carleson. The dynamics of the Hénon map. *Ann. of Math.*, 133:73–169, 1991.

(11) M. Benedicks and M. Viana. Solution of the basin problem for Hénon-like attractors. *Invent. Math.*, 143:375–434, 2001.

(12) M. Benedicks and L. S. Young. Sinai-Bowen-Ruelle measure for certain Hénon maps. *Invent. Math.*, 112:541–576, 1993.

(13) E. Bedford and J. Smillie. Real polynomial diffeomorphisms with maximal entropy: I. Tangencies. *Ann. of Math.*, 160:1–26, 2004.

(14) E. Bedford and J. Smillie. Real polynomial diffeomorphisms with maximal entropy: II. Small Jacobian. *Ergod. Th. & Dynam. Sys.*, 26:1259–1283, 2005.

(15) Y. Cao, S. Luzzato, and I. Rios. The boundary of hyperboliity for Hénon-like families. *Ergod. Th. & Dynam. Sys.*, 28:1049–1080, 2008.

(16) X. Zhang. Hyperbolic invariant sets of the real generalized Hénon maps. *Chaos, Solitons, Fractals*, 43:31–41, 2010.

(17) G. Leonov, N. Kuznetsov, and V. Vagaitsev. Localization of hidden Chua's attractors. *Phys. Lett. A.*, 375:2230–2233, 2011.

(18) G. Chen and T. Ueta. Yet another chaotic attractor. *Int. J. Bifurcation Chaos*, 9:1465–1466, 1999.

(19) G. Leonov and N. Kuznetsov. Hidden attractors in dynamical systems. From hidden oscillations in Hilbert-Kolmogorov, Aizerman, and Kalman problems to hidden chaotic attractor in Chua circuits. *Int. J. Bifurcation Chaos*, 23:1330002 (69 pages), 2013.

(20) G. Chen, N. Kuznetsov, G. Leonov, and T. Mokaev. Hidden attractors on one path: Glukhovsky-Dolzhansky, Lorenz, and Rabinovich systems. *Int. J. Bifurcation Chaos*, 27:1750115 (9 pages), 2017.

(21) S. Jafari, J. Sprott, and F. Nazarimehr. Recent new examples of hidden attractors. *Eur. Phys. J. Special Topics*, 224:1469–1476, 2015.

(22) M. Molaie, S Jafari, J. Sprott, and M. Golpayegani. Simple chaotic flows with one stable equilibrium. *Int. J. Bifurcation Chaos*, 23:1350188 (7 pages), 2013.

(23) J. Sprott. Some simple chaotic flows. *Phys. Rev. E*, 50:R647–R650, 1994.

(24) S. Jafari, V.-T. Pham, S. Moghtadaei, and S. Kingni. The relationship between chaotic maps and some chaotic systems with hidden attractors. *Int. J. Bifurcation Chaos*, 26:1650211 (8 pages), 2016.

(25) H. Jiang, Y. Liu, Z. Wei, and L. Zhang. Hidden chaotic attractors in a class of two-dimensional maps. *Nonlinear Dyn.*, 85:2719–2727, 2016.

(26) X. Zhang and G. Chen. Polynomial maps with hidden complex dynamics. *Discrete Continuous Dynamical Systems-B*, 24:2941–2954, 2019.

Seiya Amoh (Non-member) received the B.E., M.E. degrees from Tokushima University in 2019, 2021, respectively. He is now a Ph.D student in Graduate School of Systems Innovation Engineering, Tokushima University. He is working on nonlinear dynamical systems, bifurcation theory, and chaos theory.

Xu Zhang (Non-member) received the Ph.D. degree from the Department of Mathematics, Michigan State University, Michigan, USA, in 2016. His research interests include differential equations and dynamical systems.

Guanrong Chen (Non-member) received the MSc degree in Computer Science from Sun Yat-sen University, Guangzhou, China in 1981 and the PhD degree in Applied Mathematics from Texas A&M University, USA in 1987. Since year 2000, he has been a Chair Professor and the founding director of the "Centre for Chaos and Complex Networks" at City University of Hong Kong. Professor Chen was elected Fellow of the IEEE in 1997, awarded the 2011 Euler Gold Medal from Russia, and conferred Honorary Doctor Degrees by the Saint Petersburg State University, Russia in 2011 and by the University of Normandy, France in 2014. He is a Member of the Academy of Europe (since 2014) and a Fellow of The World Academy of Sciences (since 2015). His research interests are in the fields of complex networks, nonlinear dynamics and control systems. He is a Highly Cited Researcher in Engineering (since 2009) according to Web of Science.

Tetsushi Ueta (Non-member) received the B.E., M.E., and D.E. degrees from Tokushima University, Tokushima, Japan, in 1990, 1992, and 1996, respectively. Since 1992, he has been with the Department of Information Science and Intelligent Systems, Tokushima University. From 1998 to 1999, he was a visiting scholar at the Department of Electrical and Computer Engineering, University of Houston. Since 2009, he has been a Professor in Center for Administration of Information Technology, Tokushima University. He is an IEICE Fellow. His research interests include bifurcation problems of dynamical systems.